Received: 14 December 2023 | Accepted: 11 January 2024
Healthcare Technology Letters
DOI: 10.1049/htl2.12077

LETTER

Mixed reality guided root canal therapy

Fangjie Li[1] | **Qingying Gao**[2] | **Nengyu Wang**[2] | **Nicholas Greene**[2] | **Tianyu Song**[3] | **Omid Dianat**[4] | **Ehsan Azimi**[2]

[1]Department of Biomedical Engineering, Johns Hopkins University, Baltimore, Maryland, USA

[2]Department of Computer Science, Johns Hopkins University, Baltimore, Maryland, USA

[3]Chair for Computer Aided Medical Procedures, Technical University of Munich, Munich, Germany

[4]School of Dentistry, University of Maryland, Baltimore, Maryland, USA

Correspondence
Ehsan Azimi, Department of Computer Science, Johns Hopkins University, Baltimore, Maryland, USA.
Email: eazimi@gmail.com

Abstract

Root canal therapy (RCT) is a widely performed procedure in dentistry, with over 25 million individuals undergoing it annually. This procedure is carried out to address inflammation or infection within the root canal system of affected teeth. However, accurately aligning CT scan information with the patient's tooth has posed challenges, leading to errors in tool positioning and potential negative outcomes. To overcome these challenges, a mixed reality application is developed using an optical see-through head-mounted display (OST-HMD). The application incorporates visual cues, an augmented mirror, and dynamically updated multi-view CT slices to address depth perception issues and achieve accurate tooth localization, comprehensive canal exploration, and prevention of perforation during RCT. Through the preliminary experimental assessment, significant improvements in the accuracy of the procedure are observed. Specifically, with the system the accuracy in position was improved from 1.4 to 0.4 mm (more than a 70% gain) using an Optical Tracker (NDI) and from 2.8 to 2.4 mm using an HMD, thereby achieving submillimeter accuracy with NDI. 6 participants were enrolled in the user study. The result of the study suggests that the average displacement on the crown plane of 1.27 ± 0.83 cm, an average depth error of 0.90 ± 0.72 cm and an average angular deviation of 1.83 ± 0.83°. Our error analysis further highlights the impact of HMD spatial localization and head motion on the registration and calibration process. Through seamless integration of CT image information with the patient's tooth, our mixed reality application assists dentists in achieving precise tool placement. This advancement in technology has the potential to elevate the quality of root canal procedures, ensuring better accuracy and enhancing overall treatment outcomes.

1 | INTRODUCTION

Endodontic treatment, commonly known as root canal therapy (RCT), is performed to address inflammation or infection within the root canal system of a tooth. RCT aims to preserve the functionality of a tooth with irreversible pulp damage. It is a technically difficult procedure in dentistry, requiring a high level of technical skill [1].

During RCT, adequate access to the pulp chamber is paramount as it directly correlates with the overall success of the endodontic procedure. Otherwise, the achievement of the RCT's objectives becomes arduous and time-consuming [2]. Research indicates that perforation occurring during access preparation can result in catastrophic mishaps, exerting detrimental effects on the long-term prognosis of the tooth [3]. The overall failure rate of accessing the pulp chamber is 20%, and the figure is significantly higher for teeth without visible root canals [1]. Moreover, identifying calcified canals presents a challenge, often leading to procedural errors such as perforation, alteration of canal geometry, and the loss of dental hard tissue [4]. Visualizing the root canal system is typically limited to radiographs [5], and most free-hand procedures are performed without direct visual guidance. However, indistinct canal paths or canals not visible on a radiograph elevate risks of mishaps during dental procedures [6]. Common procedural errors during access cavity preparation include deviated penetration points, incomplete or small access cavities, excessive dentin removal which may lead to tooth fracture under functional loads, and perforations due to incorrect drill inclination or deep penetration.

Another challenge of the RCT is reflected in its training. In a study where dental students performed RCT on phantoms, they achieved lackluster results, with only 53% of the access canals having adequate depth [7].

To mitigate the potential procedural errors, we have focused on addressing the following three critical challenges:

- **Accurate tooth localization**: By ensuring precise tooth localization, including accurate determination of the tooth's angulation and center of the cementoenamel junction (CEJ), we aim to prevent errors during the initial penetration phase with clear visual indications of the ideal angle and location on the axial sections in CBCT [8]. For example, accurate tooth localization would aid in selecting a good penetration point centered at the CEJ level and along the long axis of the tooth without being misled by any discrepancies in the crown's location.
- **Comprehensive canal exploration**: To minimize the risk of missed root canals and excessive dentin loss [9], a thorough exploration and meticulous investigation of the tooth's internal anatomy is necessary. We aim to incorporate CBCT images in our system to offer accurate geometric information [10] to enhance the evaluation of missed canals, identify root fractures, and assess iatrogenic errors such as perforation and fractured instruments.
- **Prevention of floor and wall perforation**: By employing refined techniques, we endeavour to minimize the occurrence of floor and wall perforations, caused by inappropriate angle, location, and depth of the tooltip, which can compromise the overall integrity and success of the procedure.

Guided endodontics with dynamic navigation systems (DNS) has been introduced as a novel treatment approach, particularly for teeth with pulp canal calcification [11]. It aims to locate root canals accurately and prevent root perforation. Evaluations of guided endodontics using cone beam computed tomography (CBCT) scans have demonstrated its clinical feasibility and safety [12] and it outperforms free-hand surgery, providing high localization accuracy and reducing time consumption [13].

However, the navigation systems used by guided endodontics met a significant limitation concerning depth perception [14], as visualizing three-dimensional anatomical structures on two-dimensional screens requires mental reconstruction and spatial understanding. Even on a stereo HMD like the HoloLens 2, absolute depth perception is limited. For example, virtual objects displayed on the HMD often have the sensation of appearing farther than they are while in a stationary position. Such distance mismatches indicate that avoiding overlaying the virtual objects, like volume and anatomies, directly onto the real objects could be a better way to mitigate the risk of depth perception errors as well as eliminate occlusion of sight and distraction from the surgical site.

By addressing these specific areas of concern, our research aims to contribute to developing an accurate and practical MR-guided navigation application to assist dentists in achieving precise tool placement and enhancing the overall success rate of RCT.

2 | BACKGROUND

2.1 | Surgical navigation system and limitations

Navigation systems play a pivotal role in modern surgical procedures by providing real-time guidance and visualization of patient-specific information. By integrating advanced tracking systems and software tools, these systems enable surgeons to align preoperative imaging data, such as CT scans [15, 16], MRI scans, or ultrasound [17], with the patient's anatomy during the surgical intervention [18, 19].

Compared to conventional freehand techniques, The utilization of surgical navigation systems in modern surgical procedures offers several benefits, including enhanced precision with real-time guidance [16, 20], improved visualization of anatomical structures [21, 22], and increased surgical efficiency [17]. However, there are also limitations [14] associated with these systems.

The first limitation pertains to hand-eye coordination, where the movement of surgical tools may appear differently on the screen compared to their actual movement in the surgical field. This discrepancy can cause confusion and hinder precise control [19].

The second limitation involves the need for surgeons to frequently shift their focus between the screen displaying augmented information and the actual surgical site on the patient's body. Such frequent shifting can disrupt workflow and lead to errors. However, the use of AR HMDs has been shown to mitigate attention distraction by eliminating the need for frequent eyesight shifts between different focal points [19, 23] and representing no remarkable distraction from real-world to users [24].

The third limitation concerns depth perception which is previously mentioned in Section 1. Despite the limited depth perception, inconsistent depth cues can contribute to cognitive overload, particularly for surgeons in training [25]. Additional viewpoints have been shown to mitigate depth errors in augmented reality approaches. without the need to change the user's perspective. Previous research has proposed various paradigms for the use of mirrors in AR applications to offer various views, which encompass utilizing real mirrors, screens with displays [26, 27], or generating virtual content that replicates the physical properties but in an opposite orientation [28]. Additionally, some approaches have leveraged pre-acquired pictures of the scene to generate multiple viewpoints [29] for alignment tasks. The AR platform, which can accommodate multiple reflective displays and allow users to scale and position images within their viewing frustum, was introduced to reduce 3D scale ambiguities and improve the AR scene realism [29]. There are still visual factors that might influence the subjective judgments of depth. Therefore, it is necessary to consider the combination of several visual cues, such as colour, shape, low/high fidelity, opacity [30], and shading types [31], to diminish the negative influence caused by virtual rendering.

The fourth limitation is the constraint on the freedom of surgeons' manipulations. These systems typically require rigid immobilization of the surgical area [32], limiting the range of motion and manoeuverability for the surgeon. To overcome this, there is a need for the development of portable and stable AR/MR devices, for example, head-mounted devices (HMD), that offers greater flexibility during surgical procedures [33].

2.2 | AR-based surgical navigation (AR-SN)

The field of augmented reality (AR) has witnessed significant advancements in recent years. However, applying AR in the medical field [34, 35], particularly during surgical procedures, is still an ongoing research effort due to the rigorous requirements of ergonomics and accuracy that must be met.

Considering the requirements for freedom of movement and accuracy in medical AR applications, two main types of systems have been developed: on-device tracking systems and hybrid AR systems. On-device tracking systems [36–39], such as HoloLens 2 [40], utilize the power of the device itself to capture real-world scenes, as well as to track and register virtual objects in real-time without the need for external tracking systems. These on-device tracking AR systems provide a more streamlined and efficient user experience with more manoeuverability. Contrarily, hybrid AR systems take a different approach by treating AR devices as display monitors while relying on external tracking systems to accurately track and register objects and AR devices. This combination of inside-out and outside-in components allows for highly precise pose estimation, minimizing errors to sub-millimetre levels [41].

Specifically, to precisely align virtual models with real-world objects [42], and ensure seamless integration between the virtual and physical domains, three distinct approaches to pose computation and registration have been described (Table 1). The first approach is marker-based [17, 22, 36, 43–46], where identifiable fiducial markers are attached to the physical objects to facilitate accurate tracking. These markers serve as reference points, enabling the system to precisely determine the position and orientation of the objects. The second approach is markerless [47], which relies on the extraction of features from images captured by the AR system. By analyzing these features, the system can estimate the pose of the objects without the need for physical markers. The third approach involves manual placement [48–50], whereby the user manually positions the virtual 3D model in its intended location within the real-world environment. This approach requires careful coordination and alignment to achieve accurate registration.

To enhance portability and freedom of movement in the surgical room, as well as to address the challenges associated with detecting natural marks in complex environments [50], we have opted to utilize a stand-alone AR-HMD to track tools equipped with reflective markers [52]. In this way, both patients and clinicians are unrestricted in their movements and can change their poses without concerns of occlusion or limitations. This enables a more seamless and dynamic surgical experience, providing enhanced mobility and adaptability during procedures.

2.3 | Our contribution

In this paper, we present a novel system integration of an HMD with on-device optical tracking of retro-reflective sphere-based markers, and endodontic instruments in order to provide surgical guidance for endodontic procedure in a self-contained single-device application. In particular, we have designed the UI elements to combat difficulties in AR surgical guidance, including reducing errors in depth perception and unique UI modalities that would provide guidance even when the targets are obscured by conventional MR object overlay. Lastly, our system was successful in improving the accuracy of phantom endodontic drilling tasks for an experienced dentist, highlighting the accuracy and effectiveness of the guidance system.

3 | SYSTEM DESCRIPTION

3.1 | System architecture

Our system uses the Microsoft HoloLens 2, an optical see-through, head-mounted display (HMD) both to display mixed-reality (XR) information and to track the 6DoF pose of various scene elements including the drilling tool and the patient mandible model. On-device optical marker tracking is achieved via the STTAR tracking package [52, 53] which uses the time-of-flight (ToF) depth sensor on the HMD [54] to track retro-reflective spheres which are rigidly attached to their respective objects. STTAR utilizes a Kalman filter to improve tracking stability. The HMD also runs an AR application that provides the user interface, guidance, the registration algorithms that were implemented in the Unity Game Engine.

3.2 | System workflow

The overall workflow of the system consists of pre-operative guidance planning, intra-operative registration, and intra-operative guidance (Figure 1). During pre-operative guidance planning, a CT volume of the patient's mandible is acquired and annotated with the ideal drill path and natural landmarks. During the intra-operative registration stage, the spatial transformation between the patient's anatomy and the pre-operative CT volume objects is computed. During the intra-operative guidance stage, the system provides guidance and feedback via different visual assets through the HMD (Figure 2).

3.3 | Markers and calibration rig

Before employing the system, it is necessary to build rigid markers which contain retro-reflective spheres. It is also necessary to create mounting mechanisms to rigidly attach the markers to the objects that need to be tracked. For the mandible, we designed

TABLE 1 Assessment of medical AR applications.

	Navigation System		Registration				Accuracy	
	On-device AR	Hybrid	Marker-Free	Marker-Based	Manual	Overlay	Angle (°)	Distance (mm)
Perez et al., 2021[a] [43]	✓			✓		✓	2.00	2.00
Katic et al., 2015[b] [48]		✓			✓		–	2.50
Wang et al., 2022 [17]	✓					✓	–	3.1 ± 2.99
Eom et al.,2022[a] [44]		✓		✓		✓	–	1.44 ± 1.05
Gsaxner et al.,2021[a] [45]	✓					✓	1.11	1.70
Benmahdjoub et al., 2022 [46]	✓			✓		✓	2.9 ± 2.9	2.7 ± 1.3
Haxthausen et al., 2021 [47]		✓	✓			✓	2	2
Von et al.,2022[a] [51]	✓			✓		✓	1.70	2.81
Pratt et al.,2018[a] [49]	✓				✓	✓	–	–
Incekara et al.,2018[a] [50]	✓				✓	✓	–	4.00
Ours[†]	✓			✓			**2.4**	**2.37**

aUsing HoloLens 2
bUsing NDI

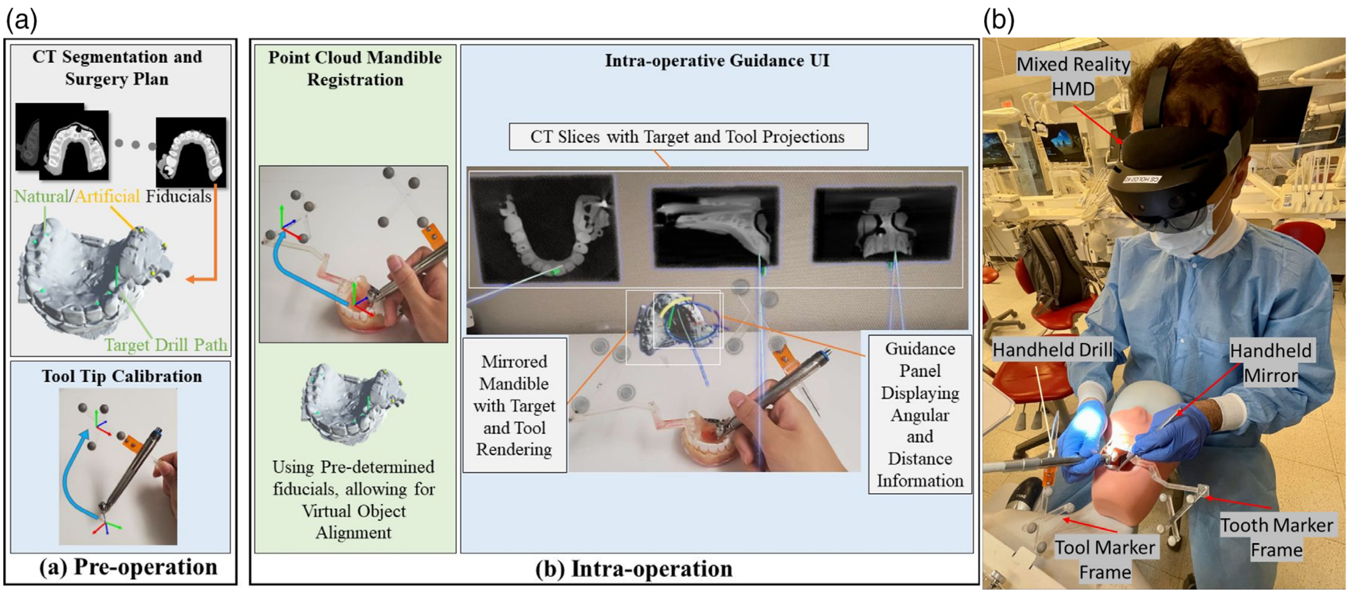

FIGURE 1 (a) The system workflow can be separated into two phases (a) Pre-operative Preparation phase, consisting of surgical planning and tool calibration (b) Intra-operative phase, consisting of patient transform registration and surgical guidance. (b) An illustration of the system setup using a dental phantom. Note that given the orientation of the patient, the view of the target site is completely obstructed, requiring the use of virtual slice and mirror displays.

a mounting mechanism by using the segmented model obtained from the pre-operative CT to create a mould. In order to achieve the necessary manufacturing accuracy, we employed the manufacturing approach of static dental guide, by using the Form 3+ Stereolithography 3D printer from Formlabs (Somerville, MA).

3.4 | Transformations: calibration and registration

In order to provide useful guidance, it is fundamentally necessary to acquire the transformation between the tooltip and target, ${}^{D}F_{VT}$, which is computed by Equation (1).

$$ {}^{D}F_{VT} = {}^{D}F_{VP}\,{}^{VP}F_{P}\,{}^{P}\mathbf{F}_{PM}\,{}^{PM}F_{HMD}\,{}^{TM}F^{-1}_{HMD}\,{}^{T}\mathbf{F}^{-1}_{TM}\,{}^{VT}F^{-1}_{T} \quad (1) $$

Within the expression, it is necessary to acquire the highlighted rigid transformations, ${}^{P}F_{PM}$ and ${}^{T}F_{TM}$, between the markers and the respective tracked objects. This is achieved in two separate steps. First, pivot calibration and manual adjustment are performed to acquire, ${}^{T}F_{TM}$, the transformation between the drill tip and the corresponding marker frame. This can be performed in advance of the operation, with the result saved by the system.

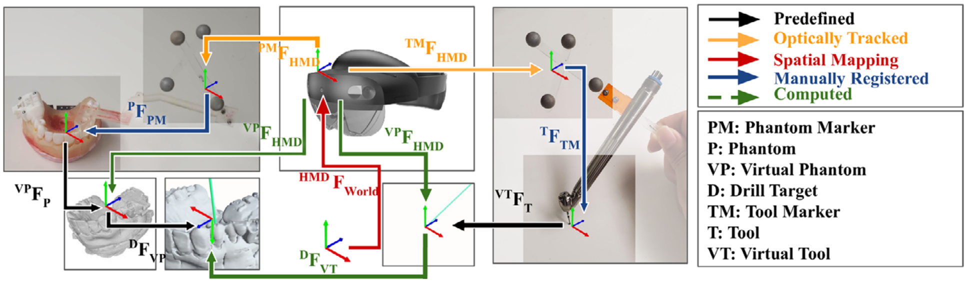

FIGURE 2 The spatial relations among the objects. It should be noted although only one virtual object pair (VP and VT) is included in the figure, it is possible to include multiple sets of virtual object pairs ({VP_i, VT_i}) for different display purposes (e.g. virtual mirrors showing coronal, sagittal, and transverse views, respectively). They would differ in the defined ${}^{P}F_{VP_i}$ and ${}^{V}F_{VT_i}$, which orients the virtual object to a desired view pose. ${}^{P}F_{PM}$ and ${}^{T}F_{TM}$, between the markers and the respectively tracked objects, need to be determined to accurately compute the transformation between the tooltip and target, ${}^{D}F_{VT}$, which is the basis of the entire guidance system.

Second, a rigid paired-point registration, based on Arun's method [55], is used to find ${}^{P}F_{PM}$, the transformation from the real mandible relative to the attached marker. During the pre-operative stage, 9 fiducial points were manually chosen along the surface of the CBCT segmentation model of the mandible model. Specifically, the points are chosen to be easily discernible natural landmarks, such as the indentations on the crowns of the teeth. For the purpose of evaluation, we also included an X-Clip impression (Figure 2) model from X-Nav Technologies (X-Nav Technologies, LLC, Lansdale, PA) during CT to add a few artificial landmarks. During the intra-operative preparation stage, the user must touch the corresponding fiducial points on the physical mandible using the calibrated drill tooltip. Finally, the paired-point registration can be completed to get the mandible position relative to the tracked marker. In practice, since the 3D-printed marker mount has a known geometry, it is possible to get a reasonably close initial estimate of the marker-mandible transformation. This initial transformation is used to overlay helpful visual cues about the landmark positions to speed up the registration process.

3.5 | User interface

The goal of our user interface is to address the limitations of depth perception and the three critical challenges of RCT which are previously outlined in Section 1.

Our UI contains three major features: virtual mirrors, dynamic CT slices, and a novel guidance method, all of which are described below.

3.5.1 | Virtual mirror

Challenge of depth perception: The limitations of depth perception in HMDs contribute not only to mental workload but also to subjective errors in judging depth between virtual-to-virtual and virtual-to-real objects.

It was previously demonstrated that the incorporation of additional viewpoints can address depth errors in egocentric AR without changing the user's perspectives. The method employed is displaying a mirrored copy of the volumetric CT mandible model, simulating a real mirror. we converted CT scans to a real-size tooth mesh [80.02 × 80.02 × 50.17 mm] and mirrored both the tooth and tooltip to face the clinicians.

Furthermore, considering the depth influence caused by a combination of visual cues within users' field of view (FOV), we set the parameters of the volumetric CT scan, the high-fidelity object (Figure 3), as opacity = 0.8, which resulted in the lowest matching error [30], and shading type = Cook–Torrance, which consisted of diffuse and specular reflections and considered subsurface reflection [31].

3.5.2 | Dynamic CT slices

Challenge of accurate tooth localization: Visualizing and accurately assessing misleading dental structures, such as the CEJ and the angle of the long axis of the target tooth, can be challenging with the naked eye alone. Moreover, insufficient visual indications of the ideal trajectory further complicate the task.

Challenge of canal exploration: Thorough analysis of CBCT plays a crucial role in preventing missed root canals and excessive dentin loss, which, if left untreated, can lead to persistent infection and subsequent inflammation.

Our application contains UI elements that show 2D CT slices (Figure 3) extracted from the pre-operative CT scans in sagittal, coronal, and axial planes in our system. These elements can be manually scaled and positioned by a user to ensure that they all simultaneously fit within the user's FOV without obstructing the real mandible. This allows the user to view this additional information without requiring frequent refocusing. Additionally, by using axial sections in CBCT, the system can detect misleading crowns and angles more efficiently, providing clear visual indications of the ideal angle and location [8].

On each of the anatomical slices, our system overlays the relative angle and distance from the current drill path to the ideal path on the CT slices. Specifically, the angular deviation is represented by a red arc (Figure 3), while the depth is

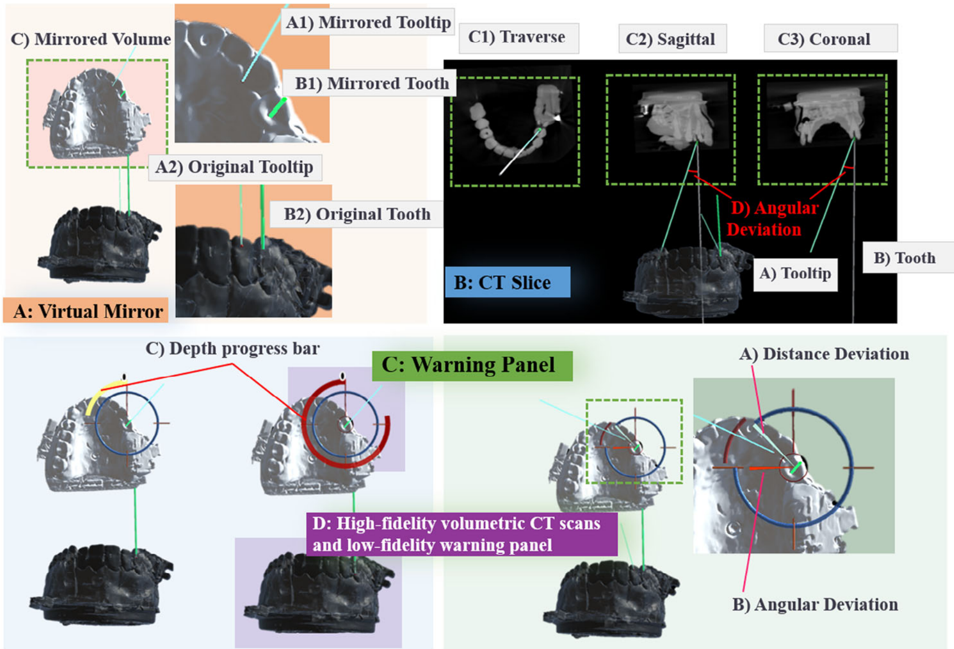

FIGURE 3 (a) Virtual mirror: a virtual mirror mirrors the real-size tooth and tooltip to face the clinicians. (b) CT slices: the CT slices contain visual indicators of angular deviation and relative location of the tool. (c) Warning panel: a scalable and movable ring-shaped warning panel displays the following information: (a) Relative distance is shown with a green pointing line. (b) Angular deviation is shown with an arc of the ring and a red pointer, and (c) Depth is shown with a colour-coded progress bar. (d) Fidelity: high-fidelity objects have more perceptual differences than low-fidelity objects.

demonstrated by the projected tooltip within the background of the tooth cross-sections. Additionally, our system dynamically updates which slices are shown the CT volume based on the current location of the tooltip. This ensures that the corresponding anatomy of the target tooth is accurately represented, enhancing comprehensive canal exploration.

3.5.3 | Guidance and feedback method

Prevention of floor and wall perforation: The occurrence of floor and wall perforations, caused by inappropriate angle, location, and depth of the tooltip, can compromise the overall integrity and success of the procedure.

We designed a scalable and movable ring-shaped warning panel (Figure 3) that is attached to the tooth volume at the beginning. The guiding module consists of indicators that warn of potentially dangerous operations and actively guide the correct tooltip movements.

- **Angular deviation**: The colour-coded second ring is divided into 8 arc-shaped pieces accompanied with a red pointing line to display a more accurate direction of the tool. The projected location of the tooltip on the circle panel is demonstrated by an arc, followed by the arc turning red and changing its length to highlight the angular deviation. This means the farther the red arc moves, the larger the deviation is.
- **Relative distance**: A dynamically updating line in the circle actively guides the user toward the target position where the line length is proportional to the tooltip distance from the target position.
- **Depth**: The outermost colour-coded progress bar visually represents the relative depth of the tooltip to the horizontal plane of the target tooth. As the tooltip gets closer to the CPFD tolerance, the colour of the progress bar transitions gradually from green to red to alert the clinician.
- **Visual cues**: Depth perception is not required in the 2D warning panel, therefore we use low-fidelity structures like rings and cylinders (Figure 3) [30]. We utilize high-contrast colours to ensure that the information is easily discernible.

4 | SYSTEM EVALUATION METHOD

A major challenge encountered throughout the development of the system was the tracking accuracy of the markers. This adversely affected the quality of the guidance information. In this section, we present our methods for analyzing the tracking error of the system in addition to the end-to-end error of the system after performing the registration procedure.

4.1 | Tracking accuracy assessment

Due to the small scale of human teeth, guidance for endodontic treatment requires high precision. In our application, we are primarily concerned with the precision of the markers' tracked poses relative to each other. Object overlay accuracy, impacted

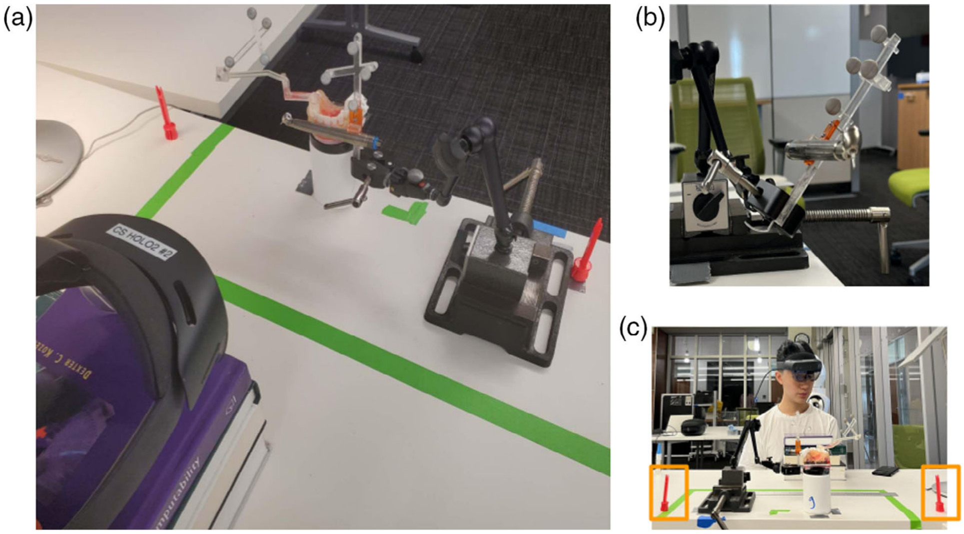

FIGURE 4 (a) General setup for evaluating the tracking accuracy of the HoloLens 2 system. (b) The setup of the tracker when tilted 45° vertically. Other rotations are done in the same manner. (c) The setup for testing the effects of head motion. The test user was instructed to shake his head and to move his view between the two markers (marked in orange boxes).

by gaze tracking accuracy, is a secondary concern because the major guidance elements in our system are the display of a virtual mirror and slice projection.

- **Tracking accuracy of the STTAR package**: We tested the accuracy of the STTAR package [52, 53]. under our setup. By using callipers and a ruler, the HoloLens 2 headset was placed on a platform 30 cm away from the tool, which had its marker in a vertical position. (Figure 4) Afterward, the tracked pose for the tool marker was recorded for 10 min at 30 Hz. The tracking variability of the stationary marker was then analyzed.
- **Impact of head motion**: As reported in past studies [48], head motion can severely affect the object-tracking accuracy of HoloLens 2. Although HoloLens 2 employs spatial mapping to correct for self-motion, given the need for the surgeon to constantly move his/her head to adjust for a better view, the residual effect can still be significant. In this regard, we let a test user wear the HoloLens 2 HMD, positioned approximately 30 cm away from the tool transform. We then marked an azimuthal ± 35 degrees arc centered around the tool transform, as shown in Figure 4. The user was instructed to sweep across the arc while rotating about only the vertical axis of the HMD to keep the tool marker in the center of the view. Using a metronome, the user repeated this motion with a frequency of 0.25 Hz for 1 min. The marker tracking variability for each test condition is reported in the next section.
- **Impact of the relative orientation of the marker**: There was a perceived reduction in tracking reliability when the marker is rotated to extreme angles. As dental treatments require the patient to be in a supine position, this is relevant. We rotated the tool marker to different orientations within ± 60 degrees both vertically and horizontally (Figure 4), whilst maintaining a 30cm distance from the HMD. The tracking result of the stationary marker was then analyzed.

4.2 | Registration and end-to-end accuracy assessment

Using nine fiducial landmarks, we performed the registration procedure for the mandible model. We computed the registration errors for the fiducial landmarks. After registration, we measured the end-to-end accuracy by using the tooltip to point to six selected landmarks as targets. The errors for these landmarks were then computed.

The same procedure was carried out using HoloLens 2 (our on-device system) and using an NDI Polaris Vicra (North Digital Inc., Waterloo, Canada) optical tracking device (hybrid system), to compare their accuracy.

We also tested the accuracy of registration using only natural landmarks, compared to using a mixture of artificial and natural landmarks. For the former, we performed registration with six natural landmarks. For the latter, performed registration 20 additional times with 6 mixed landmarks which were randomly selected each time.

5 | EXPERIMENTAL SETUP

Figure 1 represents the experimental setup for mixed reality guided procedure. The dentist is wearing Microsoft HoloLens 2 (Microsoft, USA) which tracks the handheld drill and the target tooth using the markers attached to each object.

To evaluate our system we prepared a simulated experimental setup for performing the root canal therapy. In our preliminary experiment, an experienced endodontist performed the drilling

TABLE 2 Tracking error results.

	Distance mean (mm)	Standard Deviation (mm)	Angular mean (deg)	Standard Deviation (deg)	Distance error Z-test	Angular error Z-test
Moving average filter	0.21	0.01	0.1	0.07	Smaller ($p < 0.0005$)	Smaller ($p < 0.0005$)
Default	1.06	0.53	0.56	0.48	N/A	N/A
Default (corrected for HMD localization error)	0.55	0.48	0.34	0.32	Smaller ($p < 0.0005$)	Smaller ($p < 0.0005$)
Tilted arker	0.94	0.54	0.34	0.32	Not Greater ($p > 0.05$)	Not Greater ($p > 0.05$)
Head oving	2.60	1.15	2.15	1.56	Greater ($p < 0.0005$)	Greater ($p < 0.0005$)

using both freehand and our proposed mixed reality method. For the freehand method, we followed the standard protocol based on the Guide to Clinical Endodontics recommended by the American Association of Endodontists [56]. A procedural plan was then generated. The mixed reality interface guided the dentist toward the correct path for drilling the affected tooth. After correcting the pose of the drill according to the in-situ feedback, the dentist began drilling to create the access cavity. The drilling continued until the desired depth was reached which is indicated in the interactive interface. Afterward, using a mirror, the dentist visually checks the drill path.

We also conducted another preliminary user study to evaluate the displacement on the coronal plane, the depth error, and angular deviation when drilling a hole in a dental model. 6 novices were included in the study. They performed the task on proxy 3D printed phantoms with foam material filled. This allowed them to perform the equivalence of the drilling task without having to turn on the drill, hence reducing the risk of injury. Participants received a brief training session on how to use the HoloLens 2 and were given the opportunity to familiarize themselves with the AR guidance for one trial.

6 | RESULTS

6.1 | Calibration and registration results

The results from tracking evaluation are listed in Table 2. To analyze the impact of each factor, Z-tests were performed between the error distribution of the default settings and each of the considered factors. The comparison result is listed in Table 2. Using the tracking settings with a moving average filter, we performed fiducial landmark-based point cloud registration with different selections of landmarks. The result is presented in Table 3. Our results showed a smaller registration error with natural fiducial landmarks than with mixed fiducials. (Z-test: $p < 0.05$).

We then used the registration result with 6 natural landmarks to measure the end-to-end target projection error. The distance error was 2.37 mm, and the angular deviation was 2.4°. However, when applying the identical algorithm for analysis, the NDI (0.48 mm/1.1°) exhibited notably superior performance when compared to the HoloLens. This performance disparity prompted us to explore the prospect of leveraging the parameters derived from the NDI measurements to enhance the accuracy of the HoloLens. Regrettably, these efforts did not yield the desired accuracy enhancement in the HoloLens output. This difference in results can potentially be attributed to the temporal lag exhibited by the HoloLens device, which consequently leads to a misalignment in both temporal and spatial domains. Consequently, this misalignment manifests as a mismatch between the detected location and the current spatial coordinates.

TABLE 3 Registration and end-to-end error results.

	Mean registration error (mm)	Mean end-to-end distance error (mm)	Mean end-to-end a error (°)
NDI 9 mixed artificial/natural fiducial landmarks	0.42	0.48	1.1
HoloLens 9 mixed artificial/atural fiducial landmarks	1.83	3.06	3.3
HoloLens 6 mixed artificial/atural fiducial landmarks[a]	1.78	3.14	2.8
6 atural fiducial landmarks	1.4245	2.37	2.4

a3 Natural Landmarks Randomly Sampled

6.2 | Experiment results

Inspired by evaluation metrics of works on endodontic surgeries [57, 58], we measured the deviation distance between the target trajectory and the resulting cavity in the transverse direction. For the freehand experiment, the extended direction of the root canal is treated as the target. The evaluation metric manifests the effectiveness of the system since it is a direct result of guidance and tracking systems assistance that are not available in the freehand method. A practitioner with expertise in endodontic surgery performed drilling first using the freehand and then using the mixed reality method. We demonstrate one case for each method and the quantification and qualification results of

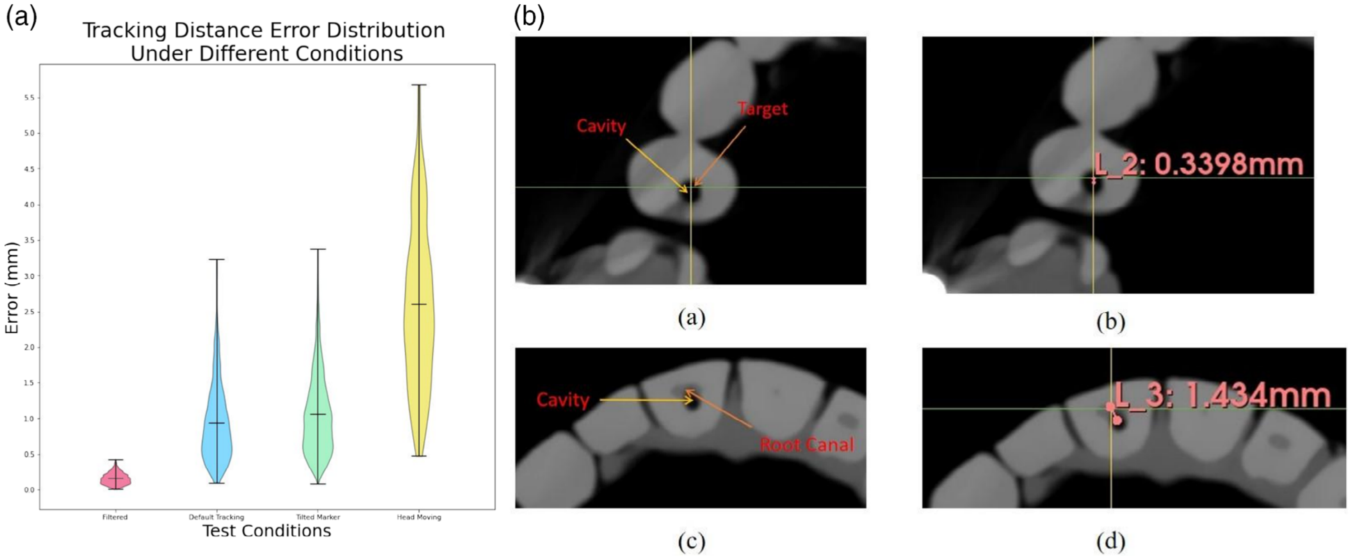

FIGURE 5 (a) The error distribution of HoloLens 2-based marker tracking using STTAR. Notice that there were significant errors induced by head motions while tilting the marker to ±60 deg had a limited impact on the error. The central dash lines are the mean errors, and the top/bottom dashes are the max/min errors. (b) (a) Transverse cross-section that shows cavity and target, where the black hole is the cavity and the cross intersection is the target. (b) The distance deviation of the cavity from the target using the mixed reality method. (c) The transverse cross-section shows the cavity and target, where the black hole is the cavity and the cross intersection is the root canal that represents the target. (d) The distance deviation of the cavity from the target using the freehand method.

the two methods are shown in Figure 5. The deviation for the mixed reality and freehand methods are 0.398 and 1.434 mm, respectively. Therefore, using the mixed reality method leads to a reduction of more than 1 mm in the error.

In the subsequent study with novice participants, each individual was instructed to use our software to guide a drilling task on a different tooth. The results showed an average displacement on the crown plane of 1.27 ± 0.83 mm, an average depth error of 0.90 ± 0.72 mm, and an average angular deviation of 1.83 ± 0.83°.

7 | DISCUSSION

7.1 | Tracking accuracy

After correcting for potential errors due to HoloLens 2 localization, the error was reduced significantly. However, this is only applicable because the device was stationary. In the case where the HMD was moving, there was greater error. This confirms the observations made by prior studies [52]. As a result, it is necessary to minimize head motion during the use of the system to improve accuracy. It may be advantageous to keep the HMD in a fixed position while performing calibration and registration when visual feedback is unnecessary. Finally, the range of marker pose changes did not significantly affect the object tracking accuracy.

7.2 | Registration and end-to-end accuracy

In our tests, the on-device HoloLens 2 and hybrid NDI external tracker-based systems achieved 2.37 and 0.48 mm end-to-end distance errors, respectively. Arguably, the reduced cost, footprint, and complexity associated with using a HoloLens 2 instead of an external tracking system can justify the reduction in accuracy, depending on the type of surgery.

In our natural vs. artificial landmark tests with the HoloLens 2, we achieved better or similar registration and end-to-end accuracy when using natural landmarks, in comparison to using mixed landmarks. This is likely because the natural landmarks on the teeth were more easily identifiable in the CT volume. Theoretically, a completely natural landmarks-based registration flow could eliminate the need for extra CT scans with artificial landmarks (e.g. X-Clip) for surgical planning, simplifying the treatment workflow and reducing extra radiation exposure.

7.3 | Value proposition and translational pathways

We engaged in extensive discussions with endodontists and dental surgeons, receiving unanimous agreement that our mixed reality solution could substantially enhance procedures, especially in complex cases.

7.3.1 | Value proposition

Conventional dynamic navigation systems, like X-Guide by X-Nav Technologies, project imaging information and guidance on an external display, requiring dentists to divert their attention from patients' teeth. This dichotomy often results in poor hand-eye coordination, potentially leading to drill placement errors. Addressing this concern, our prototype overlays augmented information directly onto the anatomy or within the field of view. Furthermore, our system offers an advantage in maintaining the user's line of sight, reducing the risk of tracking failure due to obstructed markers—a risk present with external navigation setups. The system's lightweight, portable nature promotes adaptability within constrained spaces or situations requiring dentist mobility. The immersive 3D imaging and guidance in our system surpasses the capabilities of traditional 2D monitors in existing navigation setups. Lastly, due to its minimal hardware components and integrated software, our system generally incurs lower costs than conventional navigation systems.

7.3.2 | Translational pathways

Drawing from our interviews with endodontists and surgeons, several pivotal considerations must be addressed for our system's translation to clinical bedside application:

- **Seamless clinical workflow integration**: Effective integration into the established workflow is critical. Our proposed system harmonizes considerably with the existing method 1, necessitating additional steps such as segmentation, registration, and planning, which, when thoughtfully orchestrated, may require around 10–15 min.
- **Robust tracking and registration**: To ensure clinical viability, our system's tracking must remain robust. It should withstand environmental changes and intermittent head movements without compromising efficiency. Equally important is an intuitive registration process. Anticipating advancements in optics, processing power, and the efficiency of algorithms, these limitations are anticipated to be mitigated.
- **Productization**: While our system stands as an initial prototype, rigorous validation is imperative for clinical use. Regulatory considerations demand FDA clearance. A cadaver study is being planned for real-world scenario evaluation. Upon successful completion of these stages and addressing requisite steps, the system can be implemented for patient use. Prudent considerations of customer segments and market size are essential before product deployment.

7.4 | Educational benefits

Insights gleaned from interviews with both dentists and dental faculty underscored the educational advantages of our system across various skill levels. The burgeoning trend of immersive learning in medicine finds strong support [59], with the system's 3D rendering facilitating comprehensive grasp of anatomy and potential anomalies. This technology could be instrumental in training dental residents, as faculty time becomes increasingly constrained and more involved with patients in need. Its potential dual utility for training and evaluation positions it as a valuable asset in dental education.

8 | CONCLUSIONS AND FUTURE WORK

In this paper, we investigated the feasibility of mixed reality for performing root canal therapy. We developed an application that provides feedback to the user directly on the anatomy using mixed reality head-mounted display. We conducted a preliminary experiment on a phantom. The results from our assessment indicate that an endodontist was able to perform the procedure with higher accuracy. The targeting accuracy was improved from 1.4 to 0.4 mm.

We are planning to conduct a controlled multi-user study with endodontic residents with different levels of expertise and evaluate their performance with our prototype.

AUTHOR CONTRIBUTIONS

Fangjie Lis: Investigation; methodology; validation; writing—original draft. **Qingying Gao**: Investigation; methodology; validation; writing—original draft. **Nengyu Wang**: Investigation; methodology; validation; writing—original draft. **Nicholas Greene**: Methodology; supervision; validation; writing—review & editing. **Tianyu Song**: Methodology; supervision; validation; writing—review & editing. **Omid Dianat**: Conceptualization; methodology; project administration; supervision; validation; writing—review & editing. **Ehsan Azimi**: Conceptualization; methodology; project administration and leadership; supervision; validation; writing—review & editing.

CONFLICT OF INTEREST STATEMENT

The authors declare no conflicts of interest.

DATA AVAILABILITY STATEMENT

Research data are not shared.

ORCID

Tianyu Song https://orcid.org/0000-0002-8428-9651
Ehsan Azimi https://orcid.org/0000-0003-3433-7958

REFERENCES

1. Cvek, M., Granath, L., Lundberg, M.: Failures and healing in endodontically treated non-vital anterior teeth with posttraumatically reduced pulpal lumen. Acta Odontol. Scand. 40(4), 223–228 (1982)
2. Krasner, P., Rankow, H.J., Abrams, E.S.: Access Opening and Canal Location. Endodontics Colleagues for Excellence Chicago. American Association of Endodontists, Chicago, IL (2010)
3. Ng, Y.L., Mann, V., Gulabivala, K.: A prospective study of the factors affecting outcomes of nonsurgical root canal treatment: part 1: periapical health. Int. Endod. J. 44(7), 583–609 (2011)
4. Amir, F.A., Gutmann, J.L., Witherspoon, D.E.: Calcific metamorphosis: a challenge in endodontic diagnosis and treatment. Quintessence Int. 32(6), 447–455 (2001)
5. Willershausen, B., Kasaj, A., Röhrig, B., Marroquin, B.B.: Radiographic investigation of frequency and location of root canal curvatures in human mandibular anterior incisors in vitro. J. Endod. 34(2), 152–156 (2008)
6. Martinho, F.C., Griffin, I.L., Corazza, B.J.M.: Current applications of dynamic navigation system in endodontics: a scoping review. Eur. J. Dent. 17(3), 569–586 (2023)
7. Al-Anesi, M.S., AlKhawlani, M.M., Alkheraif, A.A., Al-Basmi, A.A., Alhajj, M.N.: An audit of root canal filling quality performed by undergraduate pre-clinical dental students, yemen. BMC Med. Educ. 19(1), 350 (2019)

8. Estrela, C., Bueno, M.R., Couto, G.S., et al.: Study of root canal anatomy in human permanent teeth in a subpopulation of Brazil's center region using cone-beam computed tomography-part 1. Braz. Dent. J. 26, 530–536 (2015)
9. Estrela, C., Pécora, J.D., Estrela, C.R., et al.: Common operative procedural errors and clinical factors associated with root canal treatment. Braz. Dent. J. 28, 179–190 (2017)
10. Shemesh, H., Cohenca, N.: Clinical applications of cone beam computed tomography in endodontics: a comprehensive review. Quintessence Int. 46, 657–668 (2015)
11. Jain, S.D., Saunders, M.W., Carrico, C.K., Jadhav, A., Deeb, J.G., Myers, G.L.: Dynamically navigated versus freehand access cavity preparation: a comparative study on substance loss using simulated calcified canals. J. Endod. 46(11), 1745–1751 (2020)
12. Ramanathan, S., Solete, P.: Cone-beam computed tomography evaluation of root canal preparation using various rotary instruments: an in vitro study. J. Contemp. Dent. Pract. 16(11), 869–872 (2015)
13. Dianat, O., Nosrat, A., Tordik, P.A., et al.: Accuracy and efficiency of a dynamic navigation system for locating calcified canals. J. Endod. 46(11), 1719–1725 (2020)
14. Mezger, U., Jendrewski, C., Bartels, M.: Navigation in surgery. Langenbeck's Arch. Surg. 398, 501–514 (2013)
15. Ma, L., Jiang, W., Zhang, B., et al.: Augmented reality surgical navigation with accurate CBCT-patient registration for dental implant placement. Med. Biol. Eng. Comput. 57, 47–57 (2019)
16. Azimi, E., Niu, Z., Stiber, M., et al.: An interactive mixed reality platform for bedside surgical procedures. In: International Conference on Medical Image Computing and Computer-Assisted Intervention, pp. 65–75. Springer, Cham (2020).
17. Wang, L., Zhao, Z., Wang, G., et al.: Application of a three-dimensional visualization model in intraoperative guidance of percutaneous nephrolithotomy. Int. J. Urol. 29(8), 838–844 (2022)
18. Chotanaphuti, T., Ongnamthip, P., Teeraleekul, K., Kraturerk, C.: Comparative study between computer assisted-navigation and conventional technique in minimally invasive surgery total knee arthroplasty, prospective control study. J. Med. Assoc. Thai 91(9), 1382–1388 (2008)
19. Azimi, E., Doswell, J., Kazanzides, P.: Augmented reality goggles with an integrated tracking system for navigation in neurosurgery. In: 2012 IEEE Virtual Reality Workshops (VRW), pp. 123–124. IEEE, Piscataway, NJ (2012)
20. Miller, R.J., Bier, J.: Surgical navigation in oral implantology. Implant Dent. 15(1), 41–47 (2006)
21. Eom, S., Sykes, D., Rahimpour, S., Gorlatova, M.: Neurolens: augmented reality-based contextual guidance through surgical tool tracking in neurosurgery. In: 2022 IEEE International Symposium on Mixed and Augmented Reality (ISMAR), pp. 355–364. IEEE, Piscataway, NJ (2022)
22. Song, T., Yang, C., Dianat, O., Azimi, E.: Endodontic guided treatment using augmented reality on a head-mounted display system. Healthcare Technol. Lett. 5(5), 201–207 (2018)
23. Hu, X., Baena, Y.F.R., Cutolo, F.: Head-mounted augmented reality platform for markerless orthopaedic navigation. IEEE J. Biomed. Health. Inf. 26(2), 910–921 (2021)
24. Aromaa, S., Väätänen, A., Aaltonen, I., Goriachev, V., Helin, K., Karjalainen, J.: Awareness of the real-world environment when using augmented reality head-mounted display. Appl. Ergon. 88, 103145 (2020)
25. Azimi, E., Winkler, A., Tucker, E., et al.: Can mixed-reality improve the training of medical procedures? In: 2018 40th Annual International Conference of the IEEE Engineering in Medicine and Biology Society (EMBC), pp. 4065–4068. IEEE, Piscataway, NJ (2018)
26. Fiala, M.: Magic mirror system with hand-held and wearable augmentations. In: 2007 IEEE Virtual Reality Conference, pp. 251–254. IEEE, Piscataway, NJ (2007)
27. Latoschik, M.E., Lugrin, J.L., Roth, D.: FakeMi: a fake mirror system for avatar embodiment studies. In: Proceedings of the 22nd ACM Conference on Virtual Reality Software and Technology, pp. 73–76. ACM, New York (2016)
28. Navab, N., Feuerstein, M., Bichlmeier, C.: Laparoscopic virtual mirror new interaction paradigm for monitor based augmented reality. In: 2007 IEEE Virtual Reality Conference, pp. 43–50. IEEE, Piscataway, NJ (2007)
29. Sukan, M., Feiner, S., Tversky, B., Energin, S.: Quick viewpoint switching for manipulating virtual objects in hand-held augmented reality using stored snapshots. In: 2012 IEEE International Symposium on Mixed and Augmented Reality (ISMAR), pp. 217–226. IEEE, Piscataway, NJ (2012)
30. Do, T.D., LaViola, J.J., McMahan, R.P.: The effects of object shape, fidelity, color, and luminance on depth perception in handheld mobile augmented reality. In: 2020 IEEE International Symposium on Mixed and Augmented Reality (ISMAR), pp. 64–72. IEEE, Piscataway, NJ (2020).
31. Ping, J., Thomas, B.H., Baumeister, J., Guo, J., Weng, D., Liu, Y.: Effects of shading model and opacity on depth perception in optical see-through augmented reality. J. Soc. Inf. Disp. 28(11), 892–904 (2020)
32. Koivukangas, T., Katisko, J., Koivukangas, J.P.: Technical accuracy of optical and the electromagnetic tracking systems. SpringerPlus 2(1), 1–7 (2013)
33. Chen, A.C., Hadi, M., Kazanzides, P., Azimi, E.: Mixed reality based teleoperation of surgical robotics. In: 2023 International Symposium on Medical Robotics (ISMR), pp. 1–7. IEEE, Piscataway, NJ (2023)
34. Raskar, R., Welch, G., Fuchs, H.: Spatially augmented reality. In: Augmented Reality: Placing Artificial Objects in Real Scenes, pp. 64–71. CRC Press, Boca Raton, FL (1999)
35. Azimi, E., Molina, C., Chang, A., Huang, J., Huang, C.M., Kazanzides, P.: Interactive training and operation ecosystem for surgical tasks in mixed reality. In: International Workshop on Computer-Assisted and Robotic Endoscopy, pp. 20–29. Springer, Cham (2018)
36. von Haxthausen, F., Rüger, C., Sieren, M.M., Kloeckner, R., Ernst, F.: Augmenting image-guided procedures through in situ visualization of 3D ultrasound via a head-mounted display. Sensors 23(4), 2168 (2023)
37. Sugahara, K., Koyachi, M., Koyama, Y., et al.: Mixed reality and three dimensional printed models for resection of maxillary tumor: a case report. Quant. Imaging Med. Surg. 11(5), 2187 (2021)
38. Liebmann, F., Roner, S., von Atzigen, M., et al.: Pedicle screw navigation using surface digitization on the Microsoft HoloLens. Int. J. Comput. Assist. Radiol. Surg. 14, 1157–1165 (2019)
39. Liu, Y., Azimi, E., Davé, N., Qiu, C., Yang, R., Kazanzides, P.: Augmented reality assisted orbital floor reconstruction. In: 2021 IEEE International Conference on Intelligent Reality (ICIR), pp. 25–30. IEEE, Piscataway, NJ (2021)
40. Palumbo, A.: Microsoft HoloLens 2 in medical and healthcare context: state of the art and future prospects. Sensors 22(20), 7709 (2022)
41. Wang, J., Shen, Y., Yang, S.: A practical marker-less image registration method for augmented reality oral and maxillofacial surgery. Int. J. Comput. Assist. Radiol. Surg. 14, 763–773 (2019)
42. Azimi, E., Qian, L., Navab, N., Kazanzides, P.: Alignment of the virtual scene to the tracking space of a mixed reality head-mounted display. arXiv:170305834 (2017)
43. Pérez-Pachón, L., Sharma, P., Brech, H., et al.: Effect of marker position and size on the registration accuracy of HoloLens in a non-clinical setting with implications for high-precision surgical tasks. Int. J. Comput. Assist. Radiol. Surg. 16, 955–966 (2021)
44. Eom, S., Kim, S., Rahimpour, S., Gorlatova, M.: AR-assisted surgical guidance system for ventriculostomy. In: 2022 IEEE Conference on Virtual Reality and 3D User Interfaces Abstracts and Workshops (VRW), pp. 402–405. IEEE, Piscataway, NJ (2022)
45. Gsaxner, C., Li, J., Pepe, A., Schmalstieg, D., Egger, J.: Inside-out instrument tracking for surgical navigation in augmented reality. In: VRST '21: Proceedings of the 27th ACM Symposium on Virtual Reality Software and Technology, pp. 1–11. ACM, New York (2021)
46. Benmahdjoub, M., Niessen, W.J., Wolvius, E.B., Walsum, T.v.: Multimodal markers for technology-independent integration of augmented reality devices and surgical navigation systems. Virtual Reality 26(4), 1637–1650 (2022)

47. Haxthausen, F.v., Chen, Y., Ernst, F.: Superimposing holograms on real world objects using HoloLens 2 and its depth camera. Curr. Dir. Biomed. Eng. 7, 111–115 (2021)
48. Katić, D., Spengler, P., Bodenstedt, S., et al.: A system for context-aware intraoperative augmented reality in dental implant surgery. Int. J. Comput. Assist. Radiol. Surg. 10, 101–108 (2015)
49. Pratt, P., Ives, M., Lawton, G., et al.: Through the HoloLens looking glass: augmented reality for extremity reconstruction surgery using 3D vascular models with perforating vessels. Eur. Radiol. Exp. 2, 1–7 (2018)
50. Incekara, F., Smits, M., Dirven, C., Vincent, A.: Clinical feasibility of a wearable mixed-reality device in neurosurgery. World Neurosurg. 118, e422–e427 (2018)
51. Von Haxthausen, F., Moreta-Martinez, R., Pose Díez de la Lastra, A., Pascau, J., Ernst, F.: Ultrarsound: in situ visualization of live ultrasound images using HoloLens 2. Int. J. Comput. Assist. Radiol. Surg. 17(11), 2081–2091 (2022)
52. Martin-Gomez, A., Li, H., Song, T., et al.: STTAR: surgical tool tracking using off-the-shelf augmented reality head-mounted displays. IEEE Trans. Visual Comput. Graphics 1–16 (2023). https://doi.org/10.1109/TVCG.2023.3238309.
53. Keller, A.: HoloLens 2 infrared retro-reflector tracking. https://github.com/andreaskeller96/HoloLens2-IRTracking (2023)
54. Ungureanu, D., Bogo, F., Galliani, S., et al.: HoloLens 2 research mode as a tool for computer vision research. arXiv:2008.11239 (2020)
55. Arun, K.S., Huang, T.S., Blostein, S.D.: Least-squares fitting of two 3-D point sets. IEEE Trans. Pattern Anal. Mach. Intell. 9(5), 698–700 (1987). https://doi.org/10.1109/TPAMI.1987.4767965
56. American Association Of Endodontists: Guide to clinical endodontics (2013). https://www.aae.org/specialty/clinical-resources/guide-clinical-endodontics. Accessed 20 Feb 2024
57. Calhoun, G., Montgomery, S.: The effects of four instrumentation techniques on root canal shape. J. Endod. 14(6), 273–277 (1988)
58. Deplazes, P., Peters, O., Barbakow, F.: Comparing apical preparations of root canals shaped by nickel-titanium rotary instruments and nickel–titanium hand instruments. J. Endod. 27(3), 196–202 (2001)
59. Ali, S.M., Aich, S., Athar, A., Kim, H.C.: Medical education, training and treatment using XR in healthcare. In: 2020 IEEE Conference on Virtual Reality and 3D User Interfaces Abstracts and Workshops (VRW), pp. 388–393. IEEE, Piscataway, NJ (2023)
60. Ungureanu, D., Bogo, F., Galliani, S., et al.: HoloLens 2 research mode as a tool for computer vision research. arXiv:200811239 (2020)
61. Liu, J.M., Narasimham, G., Stefanucci, J.K., Creem-Regehr, S., Bodenheimer, B.: Distance perception in modern mobile augmented reality. In: 2020 IEEE Conference on Virtual Reality and 3D User Interfaces Abstracts and Workshops (VRW), pp. 196–200. IEEE, Piscataway, NJ (2020)
62. Hoff, W., Vincent, T.: Analysis of head pose accuracy in augmented reality. IEEE Trans. Visual Comput. Graph. 6(4), 319–334 (2000). https://doi.org/10.1109/2945.895877
63. Wu, X., Taylor, R.H.: A framework for calibration of electromagnetic surgical navigation system. In: Proceedings of the 2003 IEEE/RSJ International Conference on Intelligent Robots and Systems (IROS 2003), vol. 1, pp. 547–552. IEEE, Piscataway, NJ (2003)
64. Habib, A.A., Taha, M.I., Farah, E.M.: Methodologies used in quality assessment of root canal preparation techniques: review of the literature. J, Taibah Univ, Med, Sci 10(2), 123–131 (2015)
65. Song, T., Sommersperger, M., Baran, T.A., Seibold, M., Navab, N.: HAPPY: hip arthroscopy portal placement using augmented reality. J. Imaging 8(11), 302 (2022)
66. Gagnon, H.C., Rosales, C.S., Mileris, R., Stefanucci, J.K., Creem-Regehr, S.H., Bodenheimer, R.E.: Estimating distances in action space in augmented reality. ACM Trans. Appl. Percept. 18(2), 1–16 (2021)

How to cite this article: Li, F., Gao, Q., Wang, N., Greene, N., Song, T., Dianat, O., Azimi, E.: Mixed reality guided root canal therapy. Healthc. Technol. Lett. 11, 167–178 (2024). https://doi.org/10.1049/htl2.12077